Cell Death and Differentiation (2008) 15, 202–212

www.nature.com/cdd

Proliferative potential after DNA damage and non-homologous end joining are affected by loss of securin

JA Bernal[1,2], M Roche[2,4], C Méndez-Vidal[1,4], A Espina[1,4], M Tortolero[3] and JA Pintor-Toro*[,1]

The faithful repair of DNA damage, especially chromosomal double-strand breaks (DSBs), is crucial for genomic integrity. We have previously shown that securin interacts with the Ku70/80 heterodimer of the DSB non-homologous DNA end-joining (NHEJ) repair machinery. Here we demonstrate that securin deficiency compromises cell survival and proliferation, but only after genotoxic stress. *Securin*$^{-/-}$ cells show a significant increase in gross chromosomal rearrangements and chromatid breaks after DNA damage, and also reveal an altered pattern of end resection in an NHEJ assay in comparison with *securin*$^{+/+}$ cells. These data suggest that securin has a key role in the maintenance of genomic stability after DNA damage, thereby providing a previously unknown mechanism for regulating tumour progression.
Cell Death and Differentiation (2008) **15,** 202–212; doi:10.1038/sj.cdd.4402254; published online 26 October 2007

The gene encoding securin/PTTG1, an inhibitor of separase activity, is implicated in functional mechanisms related to cell-cycle control and tumorigenesis.[1,2] Separase function is required for sister-chromatid separation during cell division. Degradation of securin at the metaphase–anaphase transition is essential for proper chromosome segregation. A role for securin in cancer pathogenesis is supported by the observation of increased expression of securin in different tumours[3–5] and in samples under a putative metastasis programme.[6] Securin overexpression, in breast cancers, also correlates with lymph node infiltration and with a higher degree of tumour recurrence. We have shown that securin interacts with p53, represses its transcriptional activity and reduces its ability to induce cell death *in vivo*, giving insights into how some tumour cells harbouring functional p53 are resistant to chemotherapy.[7] However, the majority of tumour cells are deficient in p53 function and thus the elucidation of other mechanisms, which affect the ability of cells to proliferate after exposure to genotoxic chemotherapy in this setting, is crucial to the problem of drug resistance.

DNA repair abnormalities and genetic instability have long been considered key to the process of tumorigenesis, as evidenced by the presence of frequent chromosomal anomalies such as deletion, inversion or translocation in tumours. The DNA double-strand break (DSB) is a severe form of template damage that, if not properly repaired, can result in chromosomal rearrangements and tumour development. Mammalian cells generally repair DSBs by either the homologous recombination (HR) or the non-homologous DNA end-joining (NHEJ) pathways. HR is primarily an error-free system participating in the maintenance of genome stability, while NHEJ is error prone and thus a likely candidate pathway leading to genome rearrangement.[8,9] NHEJ repair requires the DNA-dependent protein kinase complex (DNA-PK). Mutations in genes of DNA-PK complex components lead to DSB repair deficiency, chromosomal instability and extreme sensitivity to DNA damage.[10,11] We have also shown that securin interacts *in vivo* and *in vitro* with the Ku heterodimer, the regulatory subunit of the DNA repair protein DNA-PK. The fact that the association between securin and the Ku heterodimer is disrupted and prevented by DSBs suggests that securin might play a role in the process or regulation of NHEJ[12] and affect the response of cells to the genotoxic stress induced by conventional cancer therapies.

To address these points, we began by investigating the role of securin in cellular responses to genotoxic stresses, in particular that of proliferation and then analysed the effect of securin loss on the NHEJ repair pathway. We show that *securin*-deficient cells have a significant decrease in proliferative potential after exposure to DNA-damaging agents, such as adriamycin (Adr), methyl methanesulphonate (MMS) or ionizing radiation (IR), than are wild-type cells. To define further the nature of the DNA damage response defect in *securin*-deficient cell lines, we analysed the repair of DSBs in NHEJ substrates *in vitro* and *in vivo* and showed a qualitative but not quantitative defect in the re-sealing of DSBs. Using Adr treatment as a model of DSB induction, we conclude that securin is important for chromosomal stability after genotoxin-mediated DNA damage, with possible therapeutic implications considering existing data on its deregulation in cancer.

[1]Centro Andaluz de Biología Molecular y Medicina Regenerativa, CABIMER, Isla de la Cartuja, Sevilla 41092, Spain; [2]Cancer Cell Unit, Hutchison/MRC, Cambridge, UK and [3]Departamento de Microbiología, Facultad de Biología, Universidad de Sevilla, Sevilla 41080, Spain
*Corresponding author: JA Pintor-Toro, Cell Signaling, Centro Andaluz de Biología Molecular y Medicina Regenerativa, CABIMER, Isla de la Cartuja, Sevilla 41092, Spain. Tel: +34 954467995; Fax: +34 954461664; E-mail: jose.pintor@cabimer.es
[4]These authors contributed equally to this work
Keywords: double-strand breaks; genotoxic stress; NHEJ; securin; genomic stability
Abbreviations: Adr, adriamycin; BrdU, bromodeoxyuridine; CPT, camptothecin; DSB, double-strand break; GCR, gross chromosomal rearrangement; HR, homologous recombination; IR, ionizing radiation; MMS, methyl methanesulphonate; NHEJ, non-homologous DNA end joining
Received 25.1.07; revised 17.9.07; accepted 19.9.07; Edited by M Oren; published online 26.10.07

Results

Gross chromosomal aberrations are seen in *securin*-null cells after exposure to genotoxic stress. *sec*$^{-/-}$ HCT116 cells have been reported to show defects in chromosomal segregation leading to aneuploidy.[13] However this phenotype has been since noted to revert after a short period in culture.[14] We confirm by karyotypic analysis of metaphase spreads at different points in culture (8, 12 and 20 passage) that the *sec*$^{-/-}$ cells used in our experiments have a stable chromosomal set (Figure 1a). We have previously shown that *securin* loss sensitizes cells to the chemotherapeutic agent 5-FU and the protein modulates p53 activity *in vivo* suggesting a role in DNA damage response pathways.[7] To characterize further these cellular responses to genotoxic stress, we looked at chromosomal integrity after DNA damage using the metaphase spread technique. Gross chromosomal rearrangements (GCRs) are typically formed when interactions between multiple broken DNA ends, which bear little or no homology, culminate in indiscriminate ligation of one to the other.[15] A representative metaphase of *sec*$^{-/-}$ HCT116 cells after exposure to the topoisomerase II (topo II) inhibitor Adr revealed random non-reciprocal translocations and fusions involving different chromosomes with a loss of normal morphology (mean$\pm$S.E.M.: 1.32$\pm$0.25, $n=25$) (Figure 1b). Such lesions were not induced at the same level (mean$\pm$S.E.M.: 0.45$\pm$0.27, $n=20$) in control cells treated with the same amount of Adr (Figure 1c). This Adr effect on *securin*-deficient cells was significantly different as compared to respective control cells values ($P=0.0243$, two-tailed unpaired *t*-test). At the same time, no difference was observed between number of GCRs in *sec*$^{-/-}$ HCT116 and *sec*$^{+/+}$ HCT116 without treatment ($P=0.5602$, two-tailed unpaired *t*-test).

Adr treatment differentially affects the cell cycle of *sec*$^{-/-}$ HCT116 cells. A predominant function of the DNA damage response pathway is to coordinate checkpoints that prevent progression of cells through the cell cycle in the presence

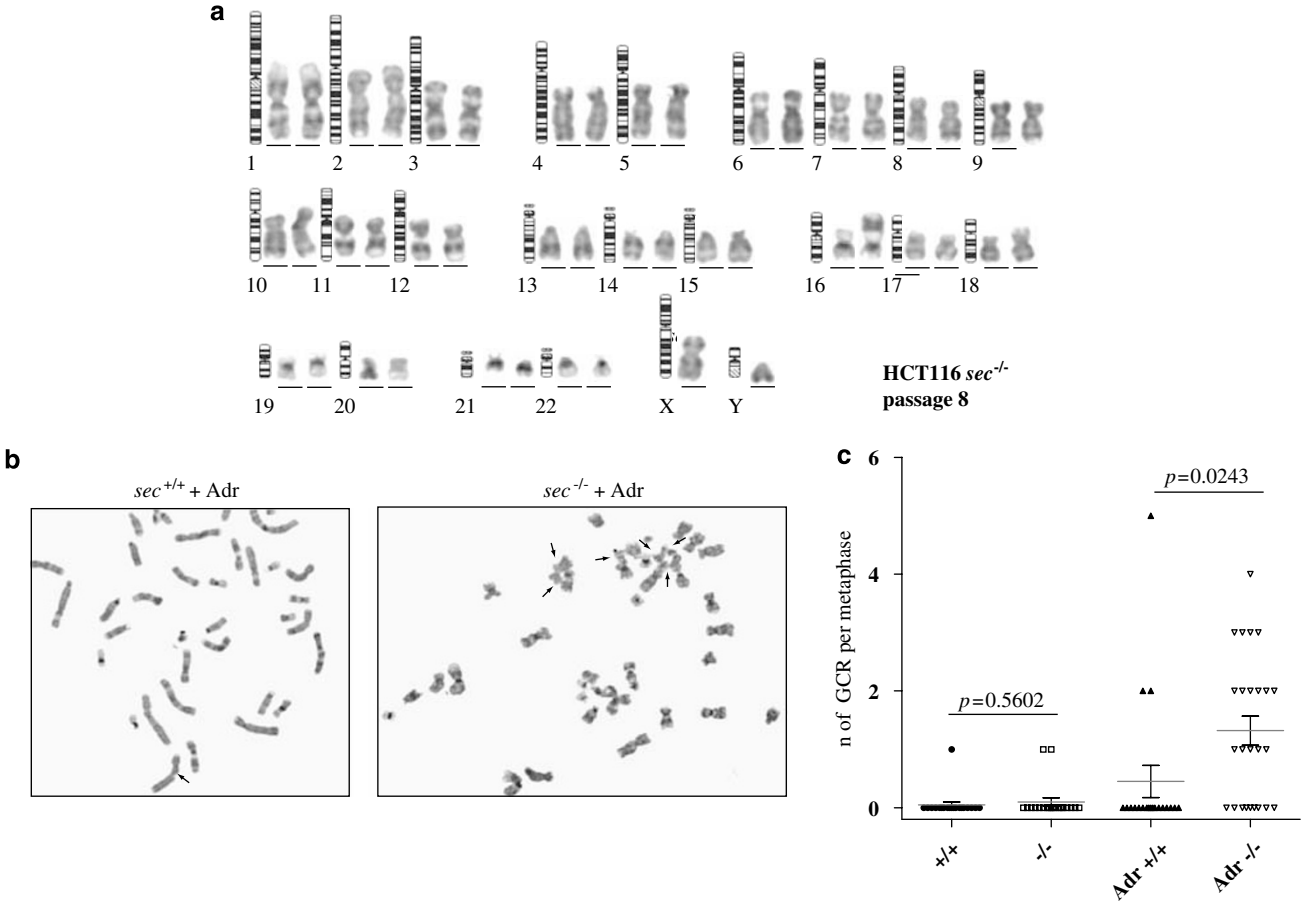

Figure 1 Genomic instability is induced after DNA damage in *securin*-deficient cells. (**a**) *securin* HCT116-deficient cells show a stable karyotype at the analysed passages 8, 12 and 20. Representative karyotype at passage 8 is shown. (**b**) Portions of two metaphase spreads from HCT116 cells after DNA damage (0.05 μg/ml Adr). The arrows indicate examples of GCRs and chromatid breaks. (**c**) Quantitative cytogenetic analysis of *sec*$^{+/+}$ HCT116 and *sec*$^{-/-}$ HCT116 cells after 0.05 μg/ml Adr treatments. Metaphase spreads were scored for the presence of GCRs. Each point in the graph represents the number of aberrations per cell; lines and error bars represent the mean and the standard error of the mean (S.E.M.) for each category respectively. The magnitude of the effect was not different between *securin*-deficient and wild-type cells without treatment (mean$\pm$S.E.M.: 0.1$\pm$0.07, $N=20$; mean$\pm$S.E.M.: 0.05$\pm$0.05, $N=20$; $P=0.5602$, two-tailed unpaired *t*-test). *sec*$^{-/-}$ HCT116 cells GCR number significantly increase after Adr treatment *versus* control (mean$\pm$S.E.M.: 1.32$\pm$0.25, $N=20$; mean$\pm$S.E.M.: 0.45$\pm$0.27, $N=20$; $P=0.0243$ two-tailed unpaired *t*-test). GCR was considered random non-reciprocal translocations and fusions involving different chromosomes

of damaged DNA. HCT116 cells are checkpoint proficient and display flow cytometric profiles characteristic of the expected G_1/S and G_2/M arrests after exposure to Adr for 72 h. Cells showed an increased sub-G_1 peak (apoptotic cells) and S phase, which suggests the existence of a viable population that has been able to repair the damaged DNA and continue along the cycle, and a second population that died after DNA damage (Figure 2a). Percentages of different cell populations treated with 0.2 μg/ml Adr in each cell-cycle phase are shown in Figure 2b. *sec*$^{-/-}$ HCT116 cells initially showed a similar response to drug treatment but began to differ by 72 h post-insult. *Securin*-deficient cells maintained the G_1 and G_2/M arrest, with a persistent suppression of DNA replication unlike their isogenic counterparts (Figure 2a and b). The decrease in number of cells re-entering S phase and mitosis after drug exposure was confirmed by bromodeoxyuridine (BrdU) incorporation and scoring of the mitotic index (Figure 2c and d). Low concentration of Adr notably arrested DNA synthesis in *sec*$^{-/-}$ HCT116 cells compared to control cells that could maintain BrdU incorporation even at 0.2 μg/ml Adr, confirming that *securin* null cells are not re-entering the cell cycle. Similarly, exposure of *securin*-deficient cells to Adr resulted in statistically significant ($P<0.0001$, two-tailed unpaired *t*-test) decrease in the percentage of mitotic cells compared to the untreated population (mean$\pm$S.E.M.: 1.6 ± 0.21, $n=1000$ *versus* mean$\pm$S.E.M.: 3.7 ± 0.28, $n=1000$) corroborating a persistent block at G_2 in *sec*$^{-/-}$ HCT116 cells. Moreover, following HCT116 cells after DNA damage using time lapse, cells do not show any mitotic feature previous to apoptotic cell death (Supplementary Figure 2). In contrast to what is observed in *securin*-deficient cells, wild-type cells showed chromatin condensation, a feature of apoptotic cells, that was prevented by the addition of z-VAD, a potent apoptosis inhibitor (Supplementary Figure 1). Consistently, under the same conditions, both PARP and caspase 3 cleavages were specifically observed in *sec*$^{+/+}$ HCT116 cells but not in *sec*$^{-/-}$ HCT116 cells, confirming that the sub-G_1 population was indeed apoptotic (Figure 2e and f). These results also indicate that apoptosis is not the cause for the decrease of *sec*$^{-/-}$ HCT116 cells in S phase after DNA damage.

***Securin*-deficiency affects the survival of cells exposed only to certain DNA-damaging agents.** The altered cell-cycle profile after DNA damage in *sec*$^{-/-}$ HCT116 cells could have effects on proliferative potential. To test this hypothesis we performed colony formation assays after exposure to different genotoxic agents. The *sec*$^{-/-}$ HCT116 cells exhibited enhanced sensitivity to Adr treatment in a dose-dependent manner when compared with wild-type HCT116 cells (Figure 3a). Similar findings were obtained after treatment with two other known genotoxins: IR and the DNA-alkylating agent MMS, highlighting the importance of the presence of securin in cell growth after DNA damage. However, when cells were grown in the presence of camptothecin (CPT), no differences between *sec*$^{-/-}$ and *sec*$^{+/+}$ cells were observed. CPT binds specifically to topo I, inducing its degradation via the proteasome. This leads to single-strand nicks on DNA that interfere with replication fork progression, inducing DSBs. The induction of DSB after these insults was confirmed by immunostaining against γ-H2AX, a known early marker for DSB response activation. Treatment with Adr, MMS and IR induced γ-H2AX foci formation in over 95% of the cells visualized (Figure 3b). CPT treatment caused less than 15% of cells to be marked as positive for DSBs. These results are in agreement with the dependence of CTP on the replication machinery to induce DSBs.

***Securin*-depleted cells show GCR and decrease viability after Adr treatment in different backgrounds.** To rule out the possibility that the results obtained were unique to HCT116 cells, U2OS human osteosarcoma cells were transfected with two independent, non-overlapping, 21 bp RNA duplexes with homology to human *securin*, and then either treated with Adr or left untreated as controls (Figure 4a and b). After incubation, a statistically significant proportion of cells with suppressed *securin* expression displayed an increase in the number of gross chromosomal abnormalities per cell *versus* U2OS control cells (mean$\pm$S.E.M.: 1.93 ± 0.29, $n=30$ *versus* mean$\pm$S.E.M.: 0.8 ± 0.24, $n=30$; $P=0.0046$, two-tailed unpaired *t*-test), confirming a role for *securin* in the maintenance of chromosomal stability after DNA damage (Figure 4c and d).

To avoid possible side effects of transient transfection of siRNAs, the *securin* gene was also inhibited in different backgrounds (HCT116, U2OS and HeLa cells) through expression of a short hairpin RNA (shRNA) complementary to *securin*, by lentivirus infection (Figure 5a). Western blot analysis showed the suppression of securin protein expression (Figure 5b). Importantly, shRNA-mediated silencing of *securin* reduces cell viability in the MTS assays in the three lines tested, HeLa, U2OS and HCT116 (Figure 5c–e). These results corroborate that low levels of securin, after Adr treatment, reduce the cell viability. To control for unexpected genetic alteration and to link cell sensitivity after DNA damage to the presence of securin, wild-type *securin* gene was reexpressed in *sec*$^{-/-}$ HCT116 cells by infecting with lentiviruses containing *securin* cDNA under the control of the *CMV* promoter. The infected cells rescued notably the Adr sensitivity observed in wild-type HCT116 cells (Figure 5e).

NHEJ is quantitatively normal in *securin*-deficient cells but occurs through aberrant end processing. The phenotypes observed by flow cytometry could be due to either a lack of repair halting the cells in the checkpoint or a downstream effect post-repair. We have previously shown that securin interacts with the Ku70-80 dimmer. This coupled to the fact that *sec*$^{-/-}$ HCT116 cells show a sensitivity profile to a particular DNA damage similar to known NHEJ proteins like Ku70 and Lig4 deficiency suggests a strong case for analysis of repair by NHEJ in these cells. This hypothesis was addressed by monitoring the DSB repair response using pulse field gel electrophoresis (PFGE) to detect the persistence of fragmented and thus unrepaired DNA over time. After irradiation with 5 Gy at different time points, only very large DNA fragments (>3.5 Mb) were observed and quantified (Figure 6b). Apoptotic DNA fragments are generally smaller than 50 kb and are clearly separated in

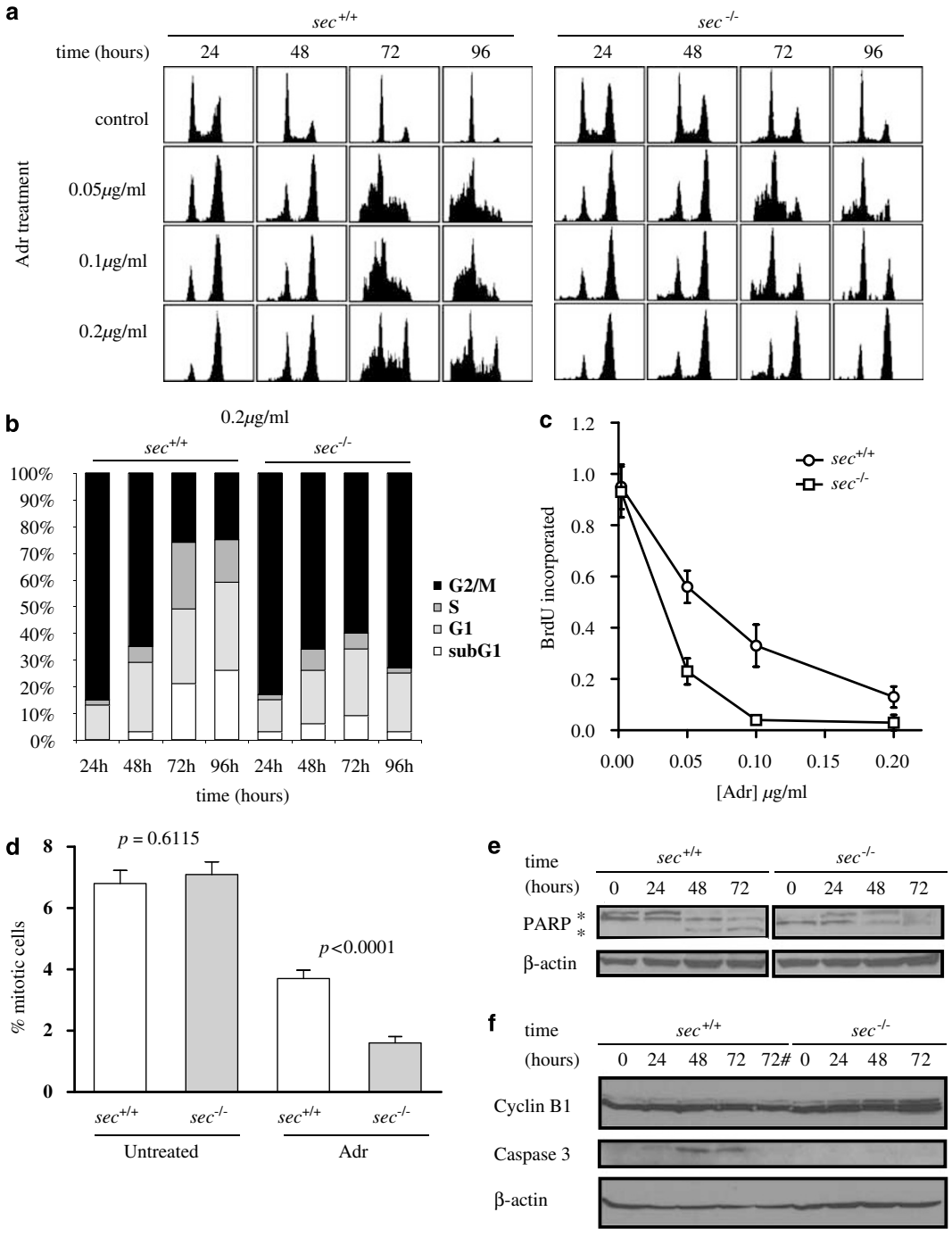

Figure 2 Growth characteristics of untreated and Adr-treated HCT116 cell lines. (**a**) DNA content histogram measured in untreated samples (control) and in cultures at different times after incubation with topo II inhibitor Adr. (**b**) Analysis of histograms in (**a**). The percentage of cells in the various cell-cycle phases is summarized for 0.2 μg/ml of Adr treatment. (**c**) Incorporation of BrdU in *sec*$^{+/+}$ HCT116 cells and *sec*$^{-/-}$ HCT116 cells after 12 h of continuous labelling. Error bars correspond to S.E.M. of three independent experiments. (**d**) Cells of the indicated genotypes were treated with 0.2 μg/ml of Adr for 3 h or left untreated. After that period, cells were allowed to recover in fresh media for 24 h before analysis. The *y* axis corresponds to the percentage of cells in mitosis (mitotic index). Error bars correspond to S.E.M. from two independent experiments. One thousand cells were analysed in each experiment. Statistical significance of the differences was tested using two-tailed *P*-value unpaired *t*-test. (**e**) Cell lysates were collected from Adr-treated cells, and immunoblots analysis performed with anti-PARP-1 antibody. Cleavage of PARP-1 was used as an apoptotic marker. β-Actin is shown as loading control. * indicates PARP-1-specific signal. (**f**) Activation of procaspase 3 was analysed as in (**e**) by immunoblotting analysis. Cyclin B1 is shown as a marker of cell cycle (maximal levels at G_2 phase). Wild-type cells were incubated with 80 μM of z-VAD apoptosis inhibitor and analysed after 72 h (line 72#) of Adr treatment

PFGE, could not be observed at these time points. In both cell lines, time course experiments show that after 4 h post-IR the bulk of DSBs do not persist, signalling that all the DNA has been resealed. Furthermore, the NHEJ repair pathway was biochemically analysed using *securin*-deficient cells nuclear extracts. A linear plasmid bearing non-matching

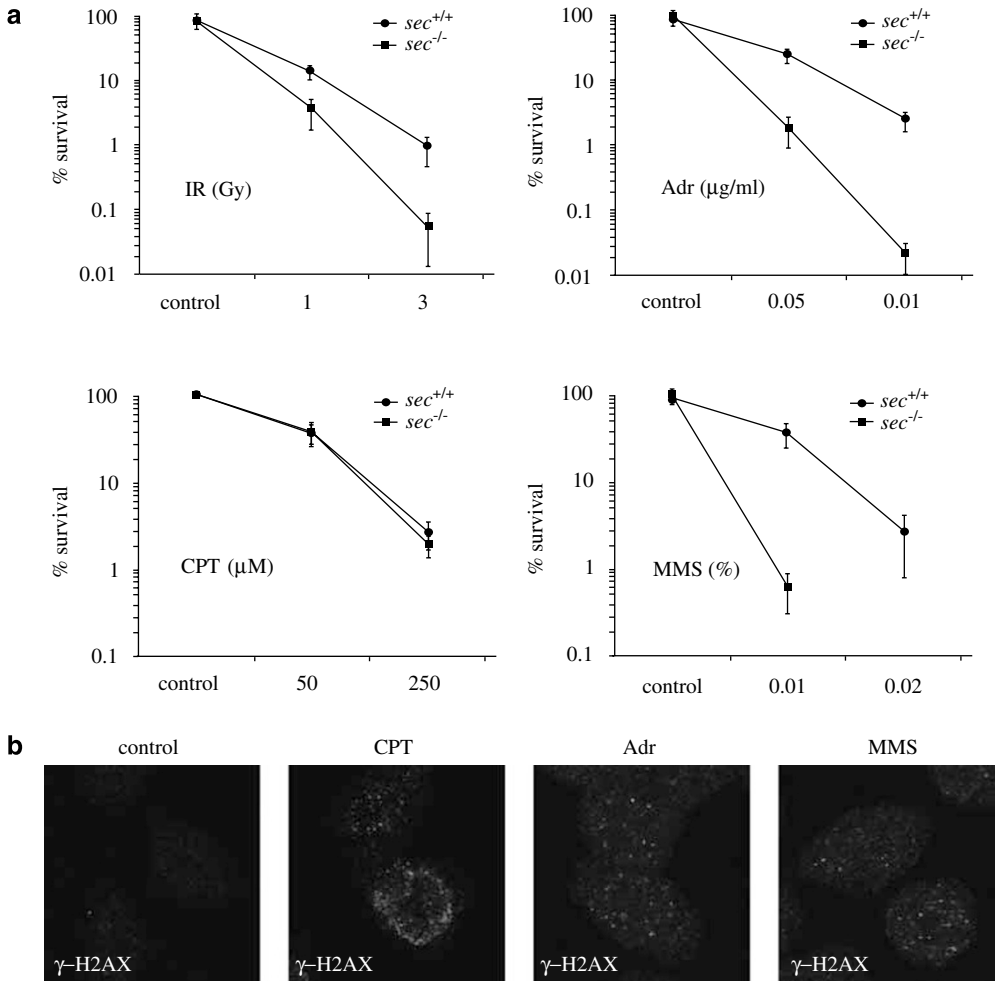

Figure 3 Sensitivity of *securin*-deficient cells to DNA-damaging agents. (**a**) Cytotoxicity induced by exposure to Adr, γ-radiation, CPT, or MMS in $sec^{-/-}$ and $sec^{+/+}$ cell lines. Data are plotted as the percentage of colonies that grew out in a given treatment over untreated cells. The plotted numbers were obtained from three independent experiments, each performed in triplicate. Error bars correspond to standard deviations. (**b**) Intracellular immunofluorescent detection of γ-H2AX in HCT116 cells after exposure to DNA damage (50 μM CPT, 0.05 μg/ml Adr and 0.01% MMS). Foci formation was detected using a confocal laser scanning microscope

*Xho*I and *Pst*I ends was used as standard NHEJ substrate (Figure 6a). Upon incubation in the $sec^{-/-}$ HCT116 nuclear extracts, this substrate underwent intramolecular NHEJ, giving rise to monomer covalently closed circles (CC). Scanning densitometry was used to quantify the bands on ethidium bromide-stained agarose gels and to determine the percentage of linear substrate that was rejoined. These experiments revealed that extracts from both cell lines efficiently rejoined the linear substrate, and no significant differences were detected, suggesting that end joining was proficient even in the absence of securin.

As the cell-extract assay is quantitative and does not detect alterations in the actual mechanism of repair, we searched for sequence changes at the site of damage as described previously.[16] The assay uses two plasmids, uncleaved *pCYCA184*, which confers chloramphenicol resistance in transformed bacteria and it is used as a transfection control, and the plasmid *pBluescript SK*$^+$ was introduced into cells as a linear fragment bearing non-matching *Xho*I and *Pst*I ends to measure NHEJ. When recovered from eukaryotic transfected cells and reintroduced into bacteria, the recircularized plasmid *pBluescript SK*$^+$ confers ampicillin resistance and serves as a quantitative measure of DNA end joining. Thus, after $sec^{-/-}$ HCT116 and $sec^{+/+}$ HCT116 cells were transfected with the two plasmids, the recovered DNA was introduced into bacteria, and the colonies plated on ampicillin and chloramphenicol plates (Figure 7a). The number of colonies obtained for the two cell lines was similar on each of the antibiotic containing plates, indicating that DNA uptake, stability and amount of end joining were similar for *securin*-deficient and *securin* wild-type cells (data not shown).

Ku80-deficient cells show an increased extent of deletion at the ends of transfected DNA in this assay.[16] To examine whether $sec^{-/-}$ HCT116 cells exhibited a similar phenotype, approximately 25 colonies were selected in each of three independent experiments, and recession length in the end-joined products was scored after sequencing the recovered plasmids (Figure 7b). In contrast to the wild type, plasmids recovered from $sec^{-/-}$ cells showed a surprisingly stark decrease in the amount of DNA deleted around the cut site, a

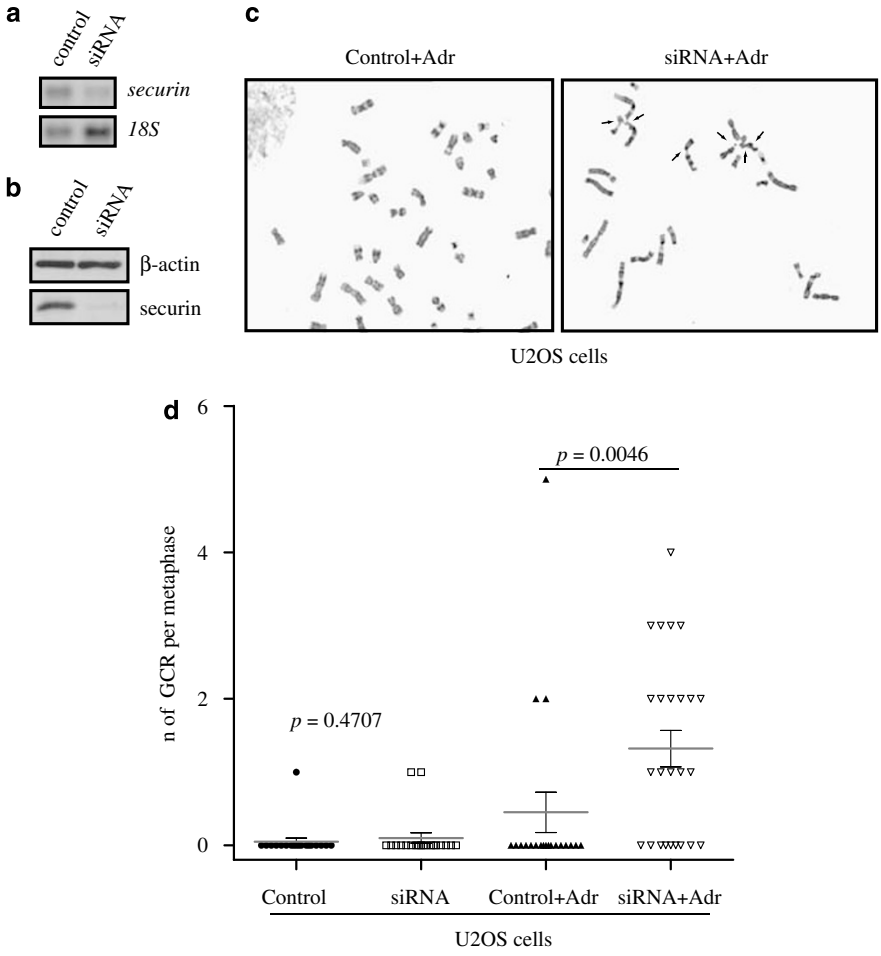

Figure 4 Genomic instability is induced in *securin* siRNA-targeted cells after DNA damage. (**a**) U2OS cells were transfected with siRNA targeting an internal sequence in the *securin* gene, harvested 24 h later and *securin* mRNA was analysed. (**b**) U2OS cells were treated with oligofectamine or transfected with *securin* siRNA. After 24 h, protein lysates were resolved and immunoblotted with anti-securin and anti-β-actin antibodies. (**c**) Comparison between control and securin protein suppressed before and after treatment with 0.05 μg/ml Adr is shown. Metaphase spreads show abnormal chromosomal structures (arrows). (**d**) Quantitative cytogenetic analysis of U2OS cells treated with oligofectamine or transfected with *securin* siRNA after 0.05 μg/ml Adr treatment. Metaphase spreads were scored for the presence of GCRs. Each point in the graph represents the number of aberrations per cell; lines and error bars represent the mean and the S.E.M. for each category respectively. The magnitude of the effect was not different between *securin*-deficient and wild-type cells without treatment (mean $\pm$ S.E.M.: 0.13 $\pm$ 0.08, $n = 30$ *versus* mean $\pm$ S.E.M.: 0.07 $\pm$ 0.046, $P = 0.4707$, two-tailed unpaired *t*-test). GCR number increases significantly after Adr treatment in *securin* siRNA-transfected cells *versus* control U2OS cells (mean $\pm$ S.E.M.: 1.93 $\pm$ 0.29, $n = 30$ *versus* mean $\pm$ S.E.M.: 0.8 $\pm$ 0.24, $P = 0.0046$, two-tailed unpaired *t*-test)

measure of resection. Thus, while wild-type cells showed repair of substrate by NHEJ with the expected end processing (69.2% $sec^{+/+}$ *versus* 16.6% in $sec^{-/-}$, $P < 0.001$, two-way ANOVA followed by Bonferroni post-test), a significant majority of plasmids in $sec^{-/-}$ cells were resealed with no end processing at all (11.5% in $sec^{+/+}$ *versus* 53.3% in $sec^{-/-}$, $P < 0.001$, two-way ANOVA followed by Bonferroni post-test), demonstrating a role for *securin* in DSB repair through NHEJ. It should be noted that overexpression of *securin* over the endogenous level in $sec^{+/+}$ HCT116 did not induce significant differences, neither in this end processing assays nor in the cell viability assays after DNA damage, compared to *securin* wild-type cells (Figure 5e and 7c). We also tested in these assays U2OS and HCT116 cells (Figure 7c and d) where *securin* was knocked down using shRNA. The results show that the abnormal end processing of DNA was not dependent on a particular cell line, but it is directly dependent on the presence of securin.

Discussion

Securin overexpression has been noted to be a common feature of several malignancies, often with a poor prognostic profile. Proliferative capacity after genotoxin exposure is a key trait in conferring chemoresistance and we demonstrate here that it is significantly reduced with loss of securin, suggesting possible driving forces behind the selection of increased protein levels in cancer. While the analysis of securin overexpression is often complicated by cell-cycle deregulation *in vitro*, our findings highlight the contribution of using genetic knockout systems to understanding the cause of its alterations in cancer.

We have previously described that the securin–Ku heterodimer interaction is affected by the induction of DSBs in DNA, suggesting a possible role for securin in the DNA damage response. Furthermore, in a recent publication McCabe and co-workers have described that overexpression of securin

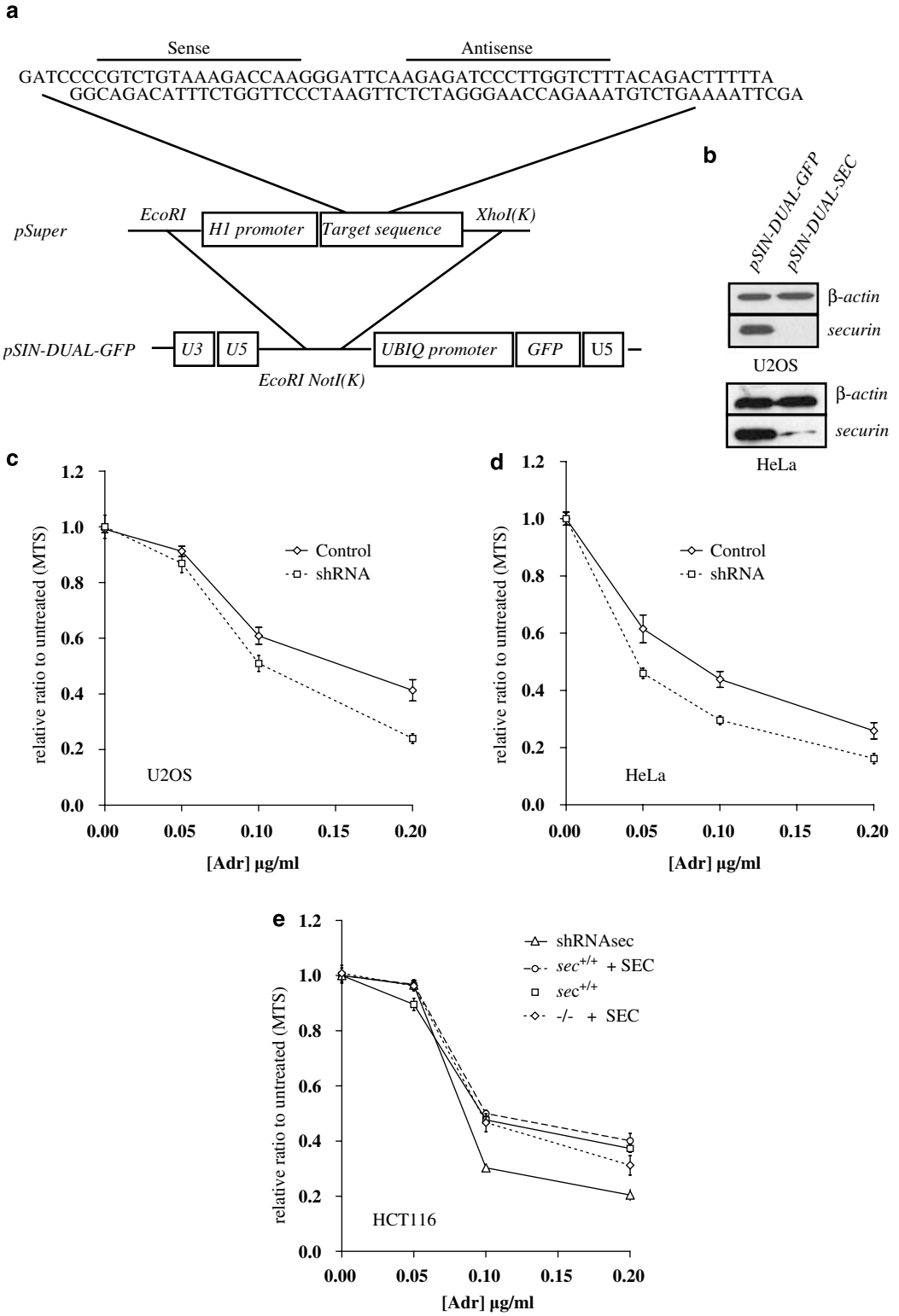

Figure 5 shRNA mediated *securin* gene supresion affects cell viability after Adr treatment. (**a**) A schematic overview of the lentiviral RNA interference vector *pSIN-DUAL-Sec*. shRNA transgene shows the sense and antisense regions that target the *securin* gene. A fragment containing the *H1* promoter and an oligonucleotide insert targeting human *securin* was excised with *Eco*RI and *Xho*I and ligated into the *pSIN-DUAL-GFP* lentiviral vector. (**b**) U2OS cells were infected with *pSIN-DUAL* control (the vector does not contain an shRNA insert) or *pSIN-DUAL-Securin*. After 72 h, protein lysates were resolved and immunoblotted with anti-securin and anti-β-actin antibodies. (**c**) Representative graph depicting decrease resistance to Adr treatment post-lentiviral infection relative to control infected U2OS cells, using MTS cell viability assays. Cells were exposed to increasing amount of Adr for 6 h and replated in fresh media, 3 days after the Adr treatment absorbance readings were normalized to the untrated values and plotted against the concentration of Adr. (**d**) Same as (**c**) after *securin* silencing in HeLa cells. (**e**) Securin was overexpressed in HCT116 wild-type cells or reexpresed in *securin*-deficient cells to study the effect of securin levels in cell viability. As before error bars represent standard deviations of the mean

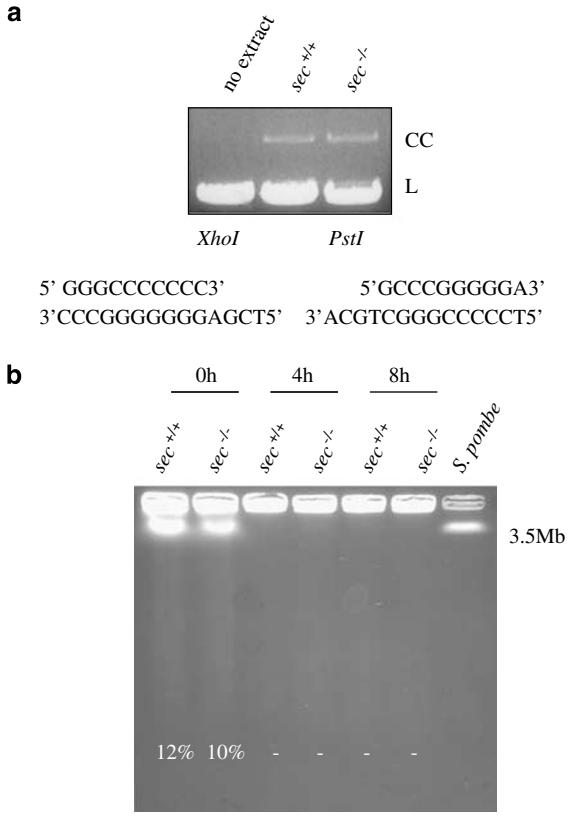

Figure 6 DNA is resealed in *securin*-deficient cells after DNA damage. (**a**) End joining of non-cohesive end DNA substrate. In this biochemical assay, L indicates the mobility of the linear substrate DNA, while CC indicates the mobility of the closed circular product. (**b**) Estimation by PFGE of chromosomal DNA DSB rejoining after γ-radiation in HCT116 cells. Cells were irradiated with 5 Gy, incubated for 0, 4 and 8 h, and subjected to PFGE. Arbitrary units represent the DNA that enters into the gel, divided by the total signal. Chromosomal *S. pombe* DNA size standards (Bio-Rad) were used in each experiment to evaluate DNA fragment size

inhibits Ku–DNA heterodimer function and decreases the extent of repair.[17] Here we add to the evidence that securin affects DNA repair after genotoxin exposure and show inaccurate repair in plasmid substrates in cells that are null for the protein.

Cells deficient in securin protein are viable with a normal cell-cycle profile under standard growth conditions.[18] This is in agreement with the observation that *securin* knock-out mice are viable and fertile.[19] However *sec*$^{-/-}$ cells are more sensitive to DSBs than are parental cells when exposed to IR, MMS or Adr, agents inducing lesions that are repaired by both HR and NHEJ, but not after exposure to CPT, which is repaired exclusively by HR.[20]

The spectrum of genotoxic sensitivity shown by *securin*-deficient cells is reminiscent of what has been described for Ku deficiency, that is to IR, MMS and Adr, but not to CPT.[21–25] The CPT-mediated DNA damage has been shown to be unique among the agents used. This agent selectively traps topo I cleavage complexes by inhibiting the religation step, thereby inducing topo I-linked DSBs. Collisions of replication forks with topo I cleavage complexes generate 'stalled fork' DSBs, which are known to be preferentially repaired by HR as opposed to NHEJ.[26–29] Our results show no differences in sensitivity to CPT of *sec*$^{-/-}$ and wild-type cells, suggesting that HR is not affected by the absence of securin.

Even though *securin*-deficient cells were proficient for resealing DSBs induced in a reporter plasmid, subtle changes at the repair site on the substrate were observed. An intriguing possibility in light of this finding and previous work on the regulation of the Ku–securin interaction by DNA damage could be that securin functions to regulate Ku heterodimer binding to DNA at DSB sites. In the absence of securin, an increase in Ku binding at the DNA ends could explain the observation of decreased resection and promoted ligation. This model is further strengthened by published data showing a reverse phenotype compared to that in *Ku*-deficient cells, with more resection before ligation.[16] The appearance of GCRs, not in proliferating cells but only after DNA damage, in cells lacking securin could thus be explained as a consequence of deregulated and therefore aberrant Ku-mediated ligation. Further biochemical work is required to elaborate on the precise mechanism of how securin affects end joining.

While *securin*-deficient cells have been proven to be unstable (loss or gain of complete chromosomes)[18] this phenotype has been shown to relapse after 2 weeks in culture.[14] It has also been noted that these cells grow normally in culture with no obvious aberrations in phenotypes such as doubling time, karyotype or cell-cycle profile, suggesting that they are a valid system for the study of DNA repair mechanisms. However, wild-type cells showed a different behaviour only after exposure to several DNA-damaging agents, as measured by a drop in number of colonies formed and appearance of GCRs. This loss in proliferative capacity after DNA damage in a *securin* deficiency background could be potentially used for targeting securin in synergy with known chemotherapeutic agents, particularly in tumours known to overexpress this protein.

Materials and Methods

Cell culture, treatments, clonogenic and viability assays. U2OS (human osteosarcoma) and HCT116 (human colorectal carcinoma) cells were purchased from ATCC. Dr. B Vogelstein kindly provided *securin*-deficient HCT116 cell line.[18] Exponentially growing cells were treated with Adr and CPT at indicated concentrations for 6 h; for MMS treatments, cells were incubated for 1 h. Immediately after treatment, cells were trypsinized and replated in new flasks with fresh media. Cells were grown for 12 days and then stained with crystal violet and counted. For viability assays, cells were plated in 96-well plates at 8000 cells/well, treated as described above, and 3 days later the relative number of viable cells were determined using the CellTiter96 Aqueous assay kit (Promega). This assay is based on cellular conversion of the tetrazolium salt, 3-(4,5-dimethylthiazol-2-yl)-5-(3-carboxymethoxyphenyl)-2-(4-sulfophenyl)-2*H*-tetrazolium (MTS) to formazan product that is soluble in culture medium and quantified by absorbance at 490 nm. Absorbance is proportional to the number of viable cells.

Construction of *securin* siRNA in lentiviral vectors. The shRNA-specific for *securin* was synthesized as two complementary DNA oligonucleotides flanked with *Bgl*II and *Hin*dIII restriction sites. The sequences were 5′- GATC CCCGTCTGTAAAGACCAAGGGATTCAAGAGATCCCTTGGTCTTTACAGACTTT TTA-3′ and 5′-AGCTTAAAAAGTCTGTAAAGACCAAGGGATCTCTTGAATCCCT TGGTCTTTACAGACGGG-3′. The underlined sequence corresponds to the targeted sequence in *securin*. Oligonucleotides were annealed and ligated into *pSuper* vector (OligoEngine), and digested with *Bgl*II and *Hin*dIII. To create the shRNA lentivirus, the siRNA cassette, containing the *H1* promoter and the hairpin siRNA sequence, was transferred from *pSUPER* to *pSIN-DUAL-GFP* by digestion of both vectors with *Xho*I and *Not*I, respectively, followed by a DNA polymerase I fill-in reaction, and a new digestion with *Eco*RI. The excised cassette was ligated into the

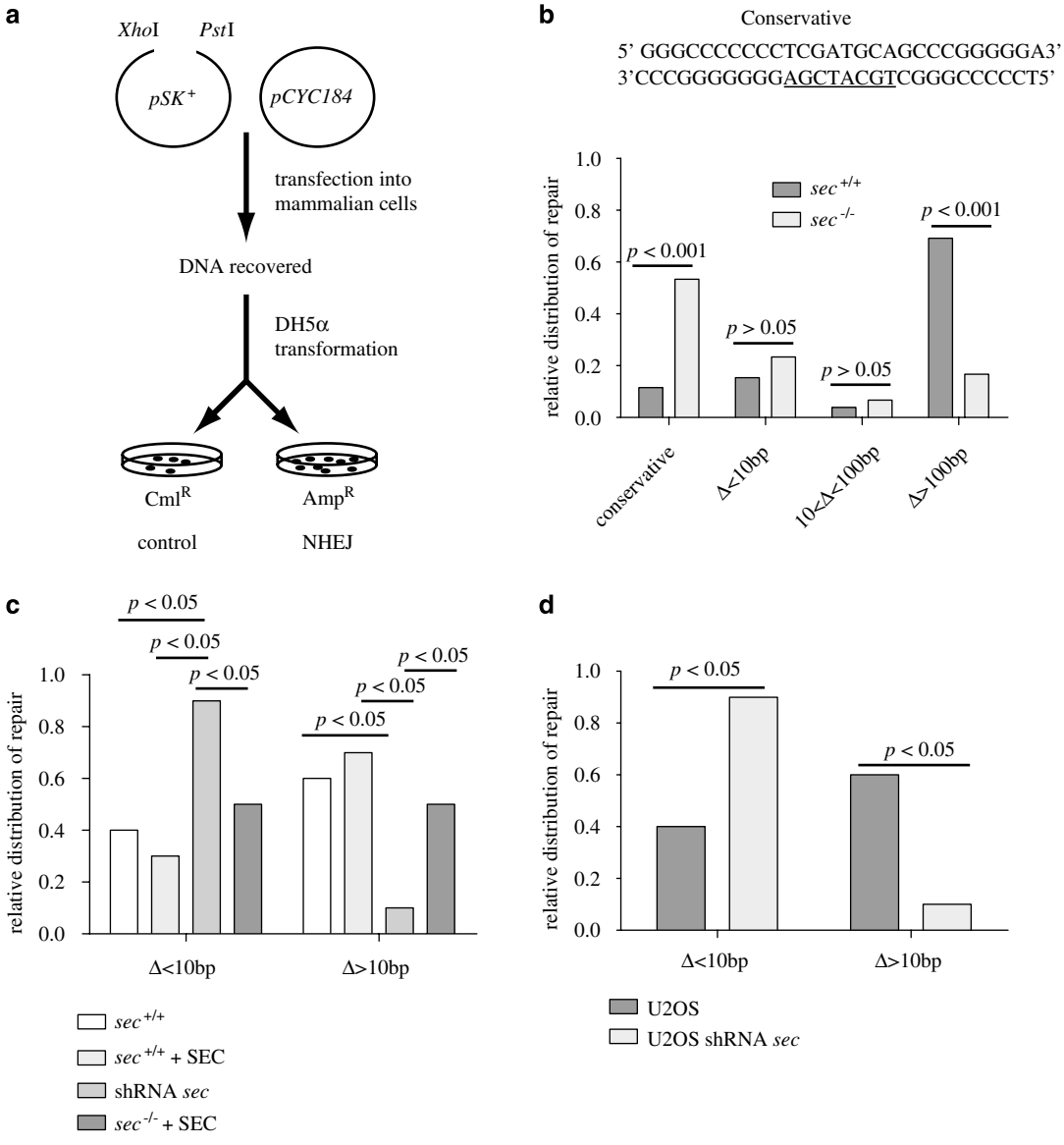

Figure 7 *sec*$^{-/-}$ cells show abnormal resection in repaired DNA. (**a**) Experimental design of NHEJ *in vivo* on extrachromosomal DNA. *pBluescript SK*$^{+}$ plasmid digested with *Pst*I and *Xho*I and uncleaved *pACYC184* plasmid were transfected into mammalian cells. Plasmid DNA was recovered after 24 h, and *E. coli* bacteria were transformed with the recovered DNA. Colonies were selected on both ampicillin (Amp) and chloramphenicol (Cml) plates. Chloramphenicol selection enables evaluation of transfection success, while ampicillin selection enables measurement of DNA end-joining activity. (**b**) Quantitation of *in vivo* extrachromosomal NHEJ assays in HCT116 wild-type and HCT116 *sec*$^{-/-}$ cell lines. DNA recovered from Amp^{R} colonies was examined for imprecise end-joint products. Input DNA sequence cleaved at *Pst*I and *Xho*I and re-joined conservatively is shown. Underlined sequence refers to the restriction/rejoining site sequence. Recovered plasmids were sequenced and scored according to the size of the deletions found around the restriction/rejoining site (conservative, $\Delta < 10$ bp, 10 bp $< \Delta <$ 100 bp and $\Delta >$100 bp). Δ indicates deletion. Differences were significant between the proportion of sequences that showed conservative resealing or resection longer than 100 bp in *securin*-deficient cells *versus* wild-type cells ($P < 0.001$, two-way ANOVA followed by Bonferroni's multiple comparison test). (**c**) Quantitative analysis of DNA end ligation assay in HCT116 cells where *securin* has been knocked down using shRNA. Recover plasmids as before were scored according to the size of the resection. In this case sequencing results were separated into two categories: deletions shorter than 10 bp ($\Delta < 10$ bp) and longer than 10bp ($\Delta >$10 bp). Significances of differences between cell lines were determined by two-way ANOVA followed by Bonferroni's multiple comparison test. Comparisons were done between HCT116 wild type infected with lentivirus delivering shRNAs against *securin* (shRNA *sec*) and the following cell lines: HCT116 wild type (*sec*$^{+/+}$), HCT116 wild type cells infected with lentivirus delivering *securin* mRNA to overexpress securin (*sec*$^{+/+}$ + *SEC*) and HCT116 *securin*-deficient cells infected with lentivirus delivering *securin* mRNA to re-express securin (*sec*$^{-/-}$ + *SEC*). (**d**) As in (**c**) U2OS cells infected with lentivirus delivering shRNA against *securin* or control infection were analysed for imprecise end-joint products. Significances of differences between cell lines were determined by two-way ANOVA followed by Bonferroni's multiple comparison test

pSIN-DUAL-GFP vector. For production of lentivirus, 10^6 293T cells were seeded onto a 10 cm Petri dish and transfected with 13.5 μg of transfer vector *pSIN-DUAL-Securin*, 9 μg of *pCMVDR8.91* and 4.5 μg of *pMDG* plasmids using Lipofectamine 2000 (Invitrogen). Lentivirus were harvested 48 h after transfection, passed through a 0.45 μm filter, and concentrated by ultracentrifugation at 20 000 r.p.m. for 2.5 h. Virus particles were dissolved in serum-free DMEM-F12 (Invitrogen), snap-frozen in liquid nitrogen and stored at -80°C. For virus titration, 2×10^5 293T cells were infected with virus plus 8 μg/ml polybrene for 6 h. Infected cells were detected by EGFP expression using a FACScan and CellQuest software (BD Biosciences).

Flow cytometry and BrdU incorporation. HCT116 cell lines were treated with Adr at different concentrations. At the indicated times, floating and adherent cells were processed for flow cytometry analysis as described.[30] DNA synthesis was assessed by BrdU incorporation for 12 h (Cell Proliferation Elisa, BrdU Colorimetric, Boehringer) in both HCT116 cell lines after 48 h of Adr incubation according to manufacturer's instructions.

siRNA-mediated *securin* silencing. *Securin* and control siRNAs consisting of 21 bp with a 2-base deoxynuneotide overhang were purchased from Proligo (France, SAS). Cells were seeded on 35 mm culture dishes and transfected with 50 nM siRNA using oligofectamine (Invitrogen) according to the manufacturer's instructions. Twenty-four hours post-transfection, RNA and protein were isolated from each dish and *securin* knockdown was validated by northern and western blot respectively. Cells stably expressing shRNA construct against *securin* mRNA were generated by lentiviral gene transfer. For infection with lentivirus stock, U2OS, HCT116 and HeLa cells were plated in 60 mm plates and incubated 2 h in their complete medium and then supplemented with lentiviral particles (MOI 0.4) and 8 μg/ml polybrene for 6 h at 37°C. Media were changed to growth media without polybrene for the rest of the experiment. Two days post-infection, cells were expanded as bulk populations.

Laser scanner confocal microscopy. Cells were grown on chamber slides, treated as indicated, and fixed in 4% paraformaldehyde in phosphate-buffered saline (PBS) for 10 min. After permeabilization in PBS + 0.05% Triton X-100 for 10 min, cells were incubated in blocking solution (5% foetal bovine serum in PBS) for 10 min. Rabbit antibodies against human γ-H2AX were obtained from Upstate Biotechnologies and used at 1 : 200 dilution in blocking solution + 0.05% Tween-20 for 1 h. Slides were then washed three times in PBS + 0.05% Tween-20 and incubated with FICT-conjugated anti-rabbit secondary antibodies at 1 : 100 for 45 min. Slides were washed as above and mounted prior to fluorescence confocal microscopy.

Immunoblot analysis. Cells were lysed in NP40 buffer (50 mM Tris-HCl pH 7.5, 150 mM NaCl, 10% glycerol, 1% (v/v) NP40) containing a complete cocktail of protease inhibitors (Roche) and 1 mM PMSF. Proteins were resolved on SDS-PAGE gels for detection of securin and β-actin. Immunoblotting was performed using the rabbit polyclonal anti-human securin described previously,[1] rabbit polyclonal anti-human PARP-1 (Roche), rabbit polyclonal anti-human caspase 3 (Cell Signaling) and monoclonal anti-human β-actin (Sigma).

Pulse field gel electrophoresis. DSB induction and repair assays have been described previously in detail.[30] Briefly, cells were irradiated and incubated at 37°C at the indicated times. Agarose plugs containing 2×10^6 cells/ml were prepared and incubated at 50°C for 38 h in lysis solution containing L-laurylsarcosine and proteinase K (Sigma-Aldrich). DNA fragment migration was resolved using pulsed-field gel electrophoresis (CHEF DRII; Bio-Rad) with a 4-day migration programme discriminating the megabase-sized fragments. Under these conditions, only fragments of <3.5 Mb are able to migrate out of the well. DSB data were expressed as the fraction of DNA fragments migrating out of the well after quantifying the light that each migration lane emitted in the ethidium bromide-stained gel using a densitometer. Chromosomal *Schizosaccharomyces pombe* DNA size standards (Bio-Rad) were used in each experiment to evaluate DNA fragment size all along the migration lane.

End-joining reactions. *In vitro* NHEJ assay was carried out using nuclear extracts prepared from *sec*$^{-/-}$ HCT116 cells or control *sec*$^{+/+}$ HCT116 cells, as described previously.[31] Circular *pBluescript SK*$^+$ plasmid DNA was linearized by restriction digestion with *Pst*I and *Xho*I to generate non-cohesive ended substrates. After restriction digest, 1 μg of linearized DNA was incubated with 5 μg of nuclear protein extract in 70 mM Tris (pH 7.5), 10 mM $MgCl_2$, 10 mM dithiothreitol and 1 mM ATP in a total volume of 50 μl for 12 h at 14°C. The reaction mixture was then treated with proteinase K at 37°C for 30 min and electrophoretically separated on a 0.8% agarose gel in Tris–borate–EDTA. Gels were scanned after staining with ethidium bromide.

Extrachromosomal DSB repair NHEJ assay. *In vivo* NHEJ assay with extrachromosomal DNA was carried out as described previously.[16] The different cell lines were transfected with plasmids, 2 μg of *pBluescript SK*$^+$ or *pEGFP* digested with *Pst*I and *Xho*I and 20 ng of uncleaved *pACYC184*, using the jetPEI™ reagent (Qbiogene). DNA was recovered from cells and reintroduced into DH5α *Escherichia coli* bacteria. The recircularized *pBluescript SK*$^+$ plasmid confers ampicillin resistance (*Amp*^{R}) and *pEGFP* plasmid confers kanamycin resistance (Kan^R), which is used as DNA end-joining measurement. Uncleaved plasmid *pACYC184* confers choramphenicol resistance (*Cmf*^{R}) to bacteria when recovered from the transfected cells and was introduced into mammalian cells as a transfection control.

Chromosomal analysis. To examine the effects of Adr treatment we used *sec*$^{-/-}$ HCT116, *sec*$^{+/+}$ HCT116 or U2OS cells expressing siRNA against *securin*. Cells were exposed to 0.05 μg/ml for 2 h and allowed to recover at 37°C for 24 h in fresh media before chromosome preparation. After recovery, cells were harvested and treated with 0.075 M KCl for 8 min at 37°C, fixed in methanol/acetic acid (3/1), spread on a glass microscope slide, air dried and Giemsa stained for GTG banding, performed as described previously.[32]

Statistical analysis. Unpaired *t*-test with two-tailed *P*-value and two-way ANOVA with Bonferroni post-test were performed using GraphPad Prism version 5.00 for Windows, GraphPadSoftware, San Diego USA (www.graphpad.com).

Acknowledgements. We are grateful to AD Jeyasekharan for helping in the English edition of the manuscript, and to B Vogelstein for HCT116 *sec*$^{-/-}$ cells, to J Sánchez for advice on chromosomal analysis and M Shivji for critical reading of the manuscript. JAP-T and MT were supported by grants from the Spanish Ministerio de Ciencia y Tecnología and the DGUI of the Junta de Andalucía. CM-V is a recipient of a postdoctoral contract (Program Juan de la Cierva) from the Spanish Ministerio de Educación y Ciencia.

1. Dominguez A, Ramos-Morales F, Romero F, Rios RM, Dreyfus F, Tortolero M *et al.* hpttg, a human homologue of rat pttg, is overexpressed in hematopoietic neoplasms. Evidence for a transcriptional activation function of hPTTG. *Oncogene* 1998; **17**: 2187–2193.
2. Zhang X, Horwitz GA, Prezant TR, Valentini A, Nakashima M, Bronstein MD *et al.* Structure, expression, and function of human pituitary tumor-transforming gene (PTTG). *Mol Endocrinol* 1999; **13**: 156–166.
3. Saez C, Japon MA, Ramos-Morales F, Romero F, Segura DI, Tortolero M *et al.* hpttg is over-expressed in pituitary adenomas and other primary epithelial neoplasias. *Oncogene* 1999; **18**: 5473–5476.
4. Heaney AP, Singson R, McCabe CJ, Nelson V, Nakashima M, Melmed S. Expression of pituitary-tumour transforming gene in colorectal tumours. *Lancet* 2000; **355**: 716–719.
5. Saez C, Martinez-Brocca MA, Castilla C, Soto A, Navarro E, Tortolero M *et al.* Prognostic significance of human pituitary tumor-transforming gene immunohistochemical expression in differentiated thyroid cancer. *The J Clin Endocrinol Metab* 2006; **91**: 1404–1409.
6. Ramaswamy S, Ross KN, Lander ES, Golub TR. A molecular signature of metastasis in primary solid tumors. *Nat Genet* 2003; **33**: 49–54.
7. Bernal JA, Luna R, Espina A, Lazaro I, Ramos-Morales F, Romero F *et al.* Human securin interacts with p53 and modulates p53-mediated transcriptional activity and apoptosis. *Nat Genet* 2002; **32**: 306–311.
8. Difilippantonio MJ, Zhu J, Chen HT, Meffre E, Nussenzweig MC, Max EE *et al.* DNA repair protein Ku80 suppresses chromosomal aberrations and malignant transformation. *Nature* 2000; **404**: 510–514.
9. Ferguson DO, Sekiguchi JM, Chang S, Frank KM, Gao Y, DePinho RA *et al.* The nonhomologous end-joining pathway of DNA repair is required for genomic stability and the suppression of translocations. *Proc Natl Acad Sci USA* 2000; **97**: 6630–6633.
10. Gu Y, Seidl KJ, Rathbun GA, Zhu C, Manis JP, van der Stoep N *et al.* Growth retardation and leaky SCID phenotype of Ku70-deficient mice. *Immunity* 1997; **7**: 653–665.
11. Gao Y, Sun Y, Frank KM, Dikkes P, Fujiwara Y, Seidl KJ *et al.* A critical role for DNA end-joining proteins in both lymphogenesis and neurogenesis. *Cell* 1998; **95**: 891–902.
12. Romero F, Multon MC, Ramos-Morales F, Dominguez A, Bernal JA, Pintor-Toro JA *et al.* Human securin, hPTTG, is associated with Ku heterodimer, the regulatory subunit of the DNA-dependent protein kinase. *Nucleic Acids Res* 2001; **29**: 1300–1307.
13. Jallepalli PV, Waizenegger IC, Bunz F, Langer S, Speicher MR, Peters JM *et al.* Securin is required for chromosomal stability in human cells. *Cell* 2001; **105**: 445–457.
14. Pfleghaar K, Heubes S, Cox J, Stemmann O, Speicher MR. Securin is not required for chromosomal stability in human cells. *PLoS Biol* 2005; **3**: e416.
15. Phillips JW, Morgan WF. Illegitimate recombination induced by DNA double-strand breaks in a mammalian chromosome. *Mol Cell Biol* 1994; **14**: 5794–5803.
16. Liang F, Jasin M. Ku80-deficient cells exhibit excess degradation of extrachromosomal DNA. *J Biol Chem* 1996; **271**: 14405–14411.
17. Kim DS, Franklyn JA, Smith VE, Stratford AL, Pemberton HN, Warfield A *et al.* Securin induces genetic instability in colorectal cancer by inhibiting double-stranded DNA repair activity. *Carcinogenesis* 2007; **28**: 749–759.
18. Jallepalli PV, Waizenegger IC, Bunz F, Langer S, Speicher MR, Peters JM *et al.* Securin is required for chromosomal stability in human cells. *Cell* 2001; **105**: 445–457.
19. Mei J, Huang X, Zhang P. Securin is not required for cellular viability, but is required for normal growth of mouse embryonic fibroblasts. *Curr Biol* 2001; **11**: 1197–1201.

20. Arnaudeau C, Lundin C, Helleday T. DNA double-strand breaks associated with replication forks are predominantly repaired by homologous recombination involving an exchange mechanism in mammalian cells. *J Mol Biol* 2001; **307**: 1235–1245.
21. Adachi N, So S, Koyama H. Loss of nonhomologous end joining confers camptothecin resistance in DT40 cells. Implications for the repair of topoisomerase I-mediated DNA damage. *J Biol Chem* 2004; **279**: 37343–37348.
22. Ninomiya Y, Suzuki K, Ishii C, Inoue H. Highly efficient gene replacements in Neurospora strains deficient for nonhomologous end-joining. *Proc Natl Acad Sci USA* 2004; **101**: 12248–12253.
23. Milne GT, Jin S, Shannon KB, Weaver DT. Mutations in two Ku homologs define a DNA end-joining repair pathway in *Saccharomyces cerevisiae*. *Mol Cell Biol* 1996; **16**: 4189–4198.
24. Ayene IS, Ford LP, Koch CJ. Ku protein targeting by Ku70 small interfering RNA enhances human cancer cell response to topoisomerase II inhibitor and gamma radiation. *Mol Cancer Ther* 2005; **4**: 529–536.
25. Gallego ME, Bleuyard JY, Daoudal-Cotterell S, Jallut N, White CI. Ku80 plays a role in non-homologous recombination but is not required for T-DNA integration in Arabidopsis. *Plant J* 2003; **35**: 557–565.
26. Pourquier P, Pommier Y. Topoisomerase I-mediated DNA damage. *Adv Cancer Res* 2001; **80**: 189–216.
27. Furuta T, Takemura H, Liao ZY, Aune GJ, Redon C, Sedelnikova OA *et al*. Phosphorylation of histone H2AX and activation of Mre11, Rad50, and Nbs1 in response to replication-dependent DNA double-strand breaks induced by mammalian DNA topoisomerase I cleavage complexes. *J Biol Chem* 2003; **278**: 20303–20312.
28. Vance JR, Wilson TE. Yeast Tdp1 and Rad1-Rad10 function as redundant pathways for repairing Top1 replicative damage. *Proc Natl Acad Sci USA* 2002; **99**: 13669–13674.
29. Nitiss J, Wang JC. DNA topoisomerase-targeting antitumor drugs can be studied in yeast. *Proc Natl Acad Sci USA* 1988; **85**: 7501–7505.
30. Foray N, Priestley A, Alsbeih G, Badie C, Capulas EP, Arlett CF *et al*. Hypersensitivity of ataxia telangiectasia fibroblasts to ionizing radiation is associated with a repair deficiency of DNA double-strand breaks. *Int J Radiat Biol* 1997; **72**: 271–283.
31. Lundberg R, Mavinakere M, Campbell C. Deficient DNA end joining activity in extracts from fanconi anemia fibroblasts. *J Biol Chem* 2001; **276**: 9543–9549.
32. Thalhammer S, Koehler U, Stark RW, Heckl WM. GTG banding pattern on human metaphase chromosomes revealed by high resolution atomic-force microscopy. *J Microsc* 2001; **202** (Part 3): 464–467.

Supplementary Information accompanies the paper on Cell Death and Differentiation website (http://www.nature.com/cdd)